Available online at www.sciencedirect.com

SCIENCE DIRECT®

Biochimica et Biophysica Acta 1667 (2004) 15–25

BIOCHIMICA ET BIOPHYSICA ACTA
BBA

http://www.elsevier.com/locate/bba

Identification of TrkA on living PC12 cells by atomic force microscopy

C.V. Gopal Reddy, Krystyna Malinowska, Nick Menhart, Rong Wang*

Department of Biological, Chemical and Physical Sciences, Illinois Institute of Technology, Chicago, IL 60616, United States

Received 3 September 2003; received in revised form 17 August 2004; accepted 26 August 2004
Available online 11 September 2004

Abstract

In neural cells, nerve growth factor (NGF) initiates its survival signal through the binding to its cell surface receptor tyrosine kinase A (TrkA). Understanding the pattern of TrkA distribution and association in living cells can provide a fingerprint for the diagnostic comparison with alterations underlying ligand–receptor dysfunction seen in various neurological diseases. In this study, we use the NGF–TrkA-specific interaction as a probe to identify TrkA on living PC12 cell by atomic force microscopy (AFM). An NGF-modified AFM tip was used to perform force volume (FV) imaging, generating a 2D force map to illustrate the distribution and association of TrkA on PC12 cell membrane. It is found that TrkA is highly aggregated at local regions of the cell. This unique protein association may be required to promote its function as a receptor of NGF. The methodology that we developed in this study can be adapted by other systems, thus providing a general tool for investigating protein association in its natural environment.

Keywords: Protein association; Living cell; Atomic force microscopy; TrkA; NGF

1. Introduction

A vast array of living functions in biological systems are mediated by ligand–receptor interactions. These interactions are in turn governed by specific protein structures, associations and distributions. While X-ray crystallography, electron microscopy and fluorescence microscopy are mature tools, atomic force microscopy (AFM) provides an alternative method in these studies. The major advantages of AFM over the other tools are that no extensive sample preparation is required and surface features of various biological samples can be examined under physiological conditions. It is well established that the AFM can be used to image living cells under physiological conditions in a nondestructive manner [1–13] and used to monitor cell response to external stimuli in real-time fashion [1,11–13]. However, protein species on cell membranes cannot be identified by topographical images alone, primarily due to the complexity of the rough cell membrane surface that consists of numbers of cell surface proteins and phospholipids. It is impossible for the AFM tip to search on the entire cell surface and identify the protein of interest by shape alone.

In addition to topographical measurement, AFM can also be operated at force mode, allowing the investigation of biorecognition by measuring the specific binding force between a biomolecular pair [14–26]. In our previous work, we studied the specific interaction between a model biomolecular pair, cholera toxin B oligomer (CTB) versus its receptor ganglioside GM1. This was achieved by monitoring the force versus separation curves in approach/retraction cycles between a GM1 functionalized tip and a CTB functionalized surface. We also used a GM1 functionalized tip to generate force maps on a CTB-containing surface that illustrated the CTB distribution [27]. With the same methodology, in this study we utilize the ligand–receptor specific interaction as a probe to search for and identify target proteins on living cell membranes. Different from a model surface, which is greatly simplified and contained only interested species, cell membrane contains diverse species. A ligand-modified AFM tip is used to perform force mapping on cell surface, generating a 2D image to demonstrate the strength of the interaction between the ligand and the cell surface species at local regions. The

* Corresponding author. Tel.: +1 312 567 3121; fax: +1 312 567 3494.
E-mail address: wangr@iit.edu (R. Wang).

0005-2736/$ - see front matter © 2004 Elsevier B.V. All rights reserved.
doi:10.1016/j.bbamem.2004.08.011

measured force is independent of surface topography, thus highlighting the distribution of the receptors which possess high affinity toward the ligand. The same strategy was employed in the recent reports on the studies of cell surface species and adhesion forces in living cells [8,28–31].

We choose to study the distribution of tyrosine kinase A (TrkA) in the living PC12 cell, a typical nerve cell. TrkA is a cell surface receptor of nerve growth factor (NGF), the best-known member of the protein family of neurotrophins involved in the development and maintenance of the peripheral and central nervous system [32–36]. NGF is a 26 kDa dimeric polypeptide [37], roughly 6×2.5×1.5 nm in size for each subunit [38] and binds two cell surface receptors: high-affinity receptor TrkA (K_d~10^{-11} M) and low-affinity receptor p75 (K_d~10^{-9} M) [37,39–41]. Binding of NGF to TrkA leads to the formation of NGF–TrkA dimer complex [33,42]. The protein kinase of each receptor monomer then phosphorylates a distinct set of tyrosine residues in the cytosolic portion of its dimer partner, which is the beginning of the signaling cascade that induces cellular proliferation, differentiation and survival. TrkA contains an extracellular portion, a single hydrophobic transmembrane α helix, and a cytosolic portion that includes a region with protein tyrosine kinase activity [32–36]. Of the five domains comprising the extracellular portion, the immunoglobulin-like domain (TrkA-d5 domain) provides the high-affinity binding site to NGF [33,36,42,43]. Since the effects of NGF are directly dependent on binding of NGF to TrkA, it is essential to understand TrkA association and distribution on the cell in order to understand NGF function in the nerve cell.

2. Materials and methods

2.1. Rat pheochromocytoma PC12 cell culture maintenance and storage

Rat pheochromocytoma PC12 cells (American Type Culture Collection, Manassas, VA) were cultured in BioCoat collagen (type I rat tail) or poly-D-lysine and laminin (mouse) coated flasks (Becton Dickinson Biosciences, Bedford, MA) in media consisting of RPMI 1640 supplemented with 5% newborn calf serum and 10% horse serum, L-glutamine, glucose and pyruvate (GIBCO™ Invitrogen Corporation, Grand Island, NY) at 37 °C in humidified incubator with 5% CO_2. Cells were maintained by splitting them every 3 days. To allow mounting in the AFM, eight-well glass culture slides (coated with laminin or collagen) cut under sterile conditions were overgrown with PC12 cells in the sterile polystyrene Petri dishes (Becton Dickinson Biosciences).

2.2. Extraction of TrkA

PC12 cells grown as above were harvested by scraping with a rubber policeman and washed with Hanks' balanced salts (Sigma, St. Louis, MO). Roughly 10^7 cells were centrifuged at 450×g for 5 min. The collected cells were extracted with 1 ml 0.1% octyl β-glucoside (Pierce Chemical Co., Rockford, IL) in 25 mM diethanolamine pH 9.0 (Fair Lawn, NJ), homogenized by 50 strokes in a Dulce homogenizer, and then sonicated with 50 3-s bursts and re-centrifuged at 12,000×g for 3 min at 4 °C. The supernatant, a crude membrane protein extraction, was analyzed by Western blotting to confirm the presence of TrkA by primary antibody (goat anti-rabbit-TrkA polyclonal; Southern Biotechnology Associates Inc., Birmingham, AL). A protein determination was done with Micro BCA™ Assay (Pierce).

The crude soluble receptors were further purified by ion exchange chromatography on a 1 ml HiTrap™ Q XL (Amersham Pharmacia, Uppsala, Sweden). Sample was applied in a buffer of 0.01% beta-octylglucoside and 25 mM diethanolamine, pH 9 and eluted with a gradient of 0–500 mM NaCl in the same buffer. TrkA, identified by Western blots, was eluted at ~100 mM NaCl. The Pharmacia fast protein liquid chromatography (FPLC) collected fractions containing approximately 25% TrkA and 75% other smaller membrane proteins were frozen in −20 °C for AFM studies.

2.3. AFM tip functionalization with NGF

We functionalized NGF onto an AFM tip using succinimidyl 3-2(2-pyridyldithio) propionate (SPDP: Molecular Probes, Eugene, OR) as a cross-linker, as reported by others [15,26], and as we routinely performed in the lab [27,44,45]. In brief, a gold-coated AFM tip, pre-cleaned by UV-ozone treatment using a tip cleaner (Bio-Force Nanosciences Inc., Ames, IA), was immersed in a 1.64×10^{-4} M SPDP solution in DMF at room temperature under N_2, generating a monolayer of self-assembled SPDP on to the tip via a thiol-gold linkage. The modified tip was rinsed with DMF, and subsequently water, and then immersed in a solution of 50 ng/ml of NGF (Sigma-Aldrich) solution (in PBS buffer) overnight at room temperature under N_2 protection. The hydroxysuccinimidyl group of SPDP, reactive toward amino acid groups on proteins [15,26,27,44,45], cross-links the NGF onto the AFM tip. The AFM tip was then thoroughly rinsed with PBS buffer and deionized water to ensure the removal of any loosely bound NGF molecule, and kept in pure water until usage.

Functionalization of proteins on a gold-coated flat silicon wafer surface was performed in a similar way, and the successful modification of a monolayer of protein was confirmed by the high-resolution AFM images of the proteins in this study and our previous studies [27,44]. These proved the effectiveness of the surface chemistry. To confirm that the NGF molecules were chemically bound on the AFM tip and they retained affinity towards the receptors, we performed force measurements between the NGF-modified tip and TrkA-modified substrate. The successful functionalization of

the tip and the substrate is evident from the reproducible and stable adhesion forces measured between the tip and the sample at many local regions. In contrast, when force curves were measured between a tip with chemically bound NGF and a substrate with physically adsorbed TrkA, or vice versa, initially frequently observed high adhesion force quickly dropped to basal level in subsequent force measurement cycles when the measurements were performed at the same region, indicative of the detachment of the non-covalently bound species. These experiments provided evidences of successful tip functionalization.

2.4. Sample preparation and AFM imaging

For AFM mounting, the square (~15 mm) laminin- or collagen-coated glass substrates overgrown with PC12 cells were glued with epoxy resin onto magnetic steel stubs of the same size. All measurements were performed within 2–4 days of seeding the slide.

All AFM measurements presented here were acquired at room temperature using a multimode Nanoscope IIIa AFM (Digital Instruments, Santa Barbara, CA), equipped with a J-type scanner in a commercially available fluid cell without O-rings. Hanks balanced salt solution (HBSS) was used as the media. The AFM was operated in fluid tapping mode for imaging using an oxide sharpened Si_3N_4 tip at a thermal resonance frequency of 8–10 kHz. Although laminin- or collagen-coated glass substrates were chosen to enhance cell adhesion, the frequency of firm cell attachment was low (as we commonly observed for PC12 cells), and it was evident that loosely adhered cells could be moving around by the AFM tip.

Force measurements were performed in fluid contact mode. Triangular Si_3N_4 cantilevers with spring constant of 0.12 nN/nm were used for the study. As schematically illustrated in Fig. 1, an NGF-modified tip was used to achieve force volume (FV) images. As this tip scanned on cell surface, force curves were obtained at each pixel. A total of 32×32=1024 force curves were collected to generate a force map. When the NGF-modified tip scanned on TrkA, a strong adhesion force is generated during tip retraction to indicate the specific interaction. The FV image illustrates the peak adhesion force along each curve at each pixel of the 2D surface. The *Z*-scan rate of the measurements was 1 Hz, and the *Z*-ramp size was typically chosen to be 500–800 nm.

To confirm the specificity of the force observed, control experiments were carried out for the same measurements in the presence of NGF (7 nM final concentration in the cell, more than 100 times the K_d of 10^{-11} M), blocking the TrkA binding sites. After 30 min incubation with NGF solution, the samples were scanned by NGF-modified AFM tip to generate FV images. The same NGF concentration was applied in the control experiments on the TrkA-modified gold substrates.

3. Results

3.1. Morphology of living cells

Images of living cells were captured in HBSS media and shown in Fig. 2. Fig. 2a shows a cell with a size of about 10 μm in diameter. The cell surface is uneven with a maximum height of 1.2 μm (measured from the simultaneously acquired height image, not shown). A dark line (arrow pointed) appears across the cell, perhaps capturing the initial stage of cell division. This cell is round in shape, and it is typical among the cells we imaged. Some of the observed cells are deviated from round shape, as shown in Fig. 2b. The shape and average size of the cells measured from AFM are consistent with the results of optical microscopic observation. Only a small portion of the cells adhered firmly enough to a collagen or laminin coated substrate to withstand the washing steps during AFM mounting. These cells were chosen for our study and can be continuously scanned up to 4 h without detachment. The images revealed rugged cell surface, with a surface roughness of 80 nm in average, which we ascribed to the cytoskeleton under the softer cell membrane, the diverse distribution and the morphology of various phospholipids and cell surface proteins. However, the individual surface features cannot be identified by topographic image alone.

3.2. Force measurements between an NGF-modified tip and a TrkA-modified substrate

To study the specific interaction between NGF and TrkA, they were chemically bound to a substrate and an AFM tip, respectively, as described in the experimental section (Section 2.3). We used the partially purified (~25%) protein solution for the substrate modification. The functionaliza-

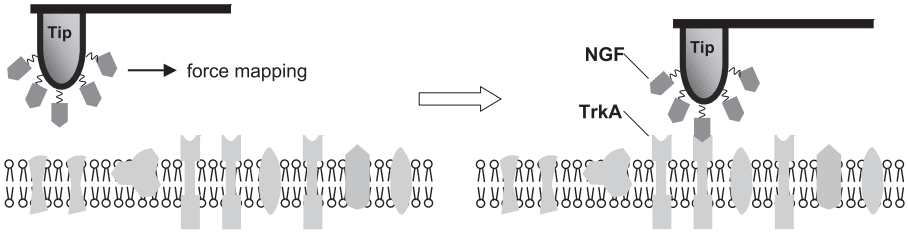

Fig. 1. Scheme of identifying TrkA receptor on PC12 cell membrane using an NGF-modified AFM tip. NGF–TrkA specific interaction was employed to identify TrkA.

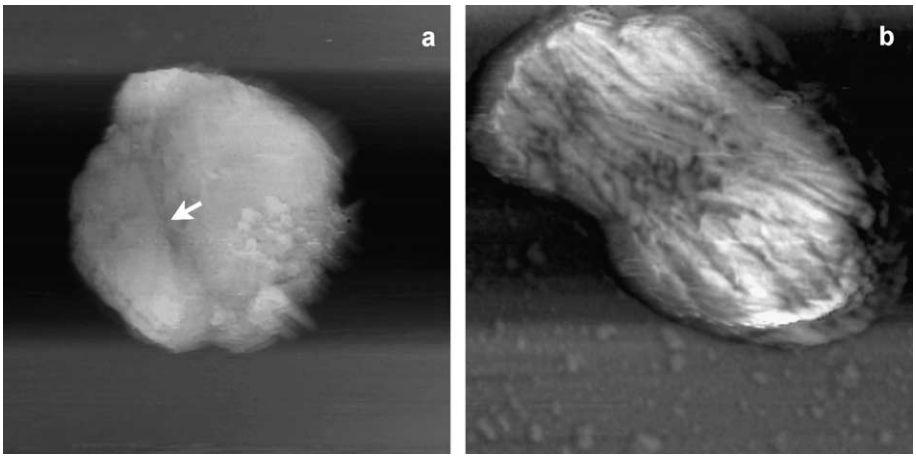

Fig. 2. Phase images of living PC12 cells captured at fluid tapping mode. Image size of panel a is 15×15 μm^2; image size of panel b is 11×11 μm^2.

tion of the gold surface was confirmed by images acquired with a bare tip. As shown in Fig. 3a, a layer of protein (bright spots, size ranges from 8 to 25 nm) uniformly and fully covers the substrate, in contrast to the flat bare substrate. The proteins were readily distinguished from the substrate in the phase image (not shown), which was captured simultaneously with the height image. The contrast between protein and substrate is analogous to our previous observations of pure proteins modified on a substrate in a similar manner [27]. It is interesting to observe that some of the proteins form pentamers and hexamers, leaving holes at the center. Though protein association might be different in a living cell, this observation provides the essential information of the tendency of protein aggregation. The height of the protein layer was measured with respect to the defect area. The most frequently measured heights are 1.5, 2.4, and 4.3 nm. This may be due to the different size and orientation of distinct proteins. Occasionally, extremely high features appear on the surface, corresponding to loosely bound species on top of the monolayer.

NGF was chemically bound onto an AFM tip as described above. Fig. 3b shows a FV image acquired

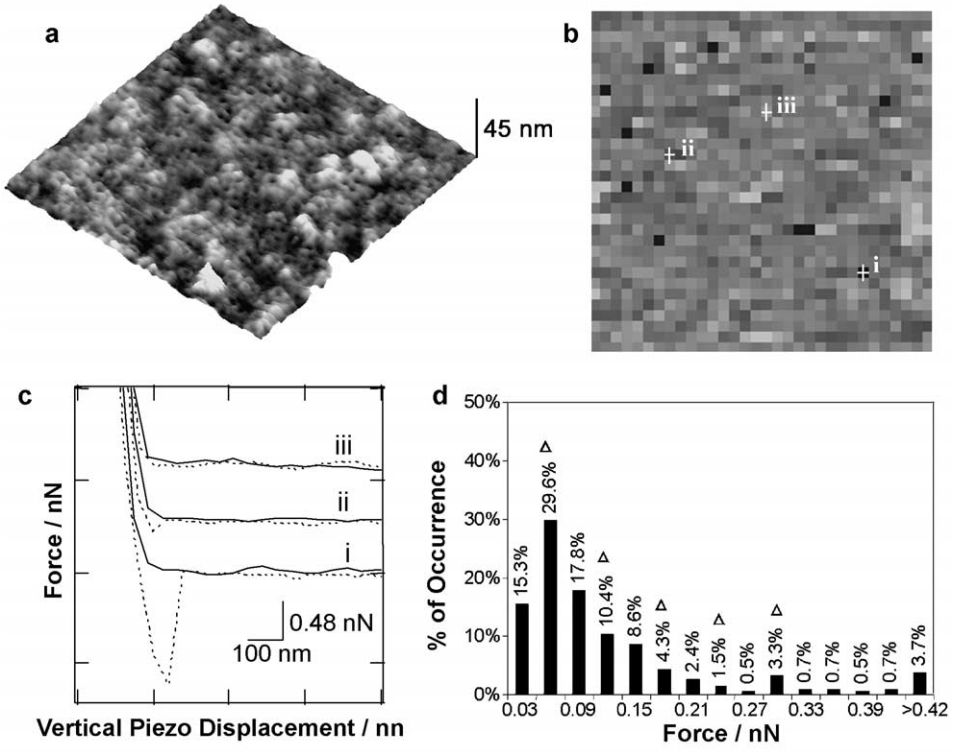

Fig. 3. (a) 3D height image of a substrate functionalized with partially purified (25% of TrkA) protein solution. The image size is 860×860 nm^2. (b) A 1×1 μm^2 FV image acquired by an NGF-modified tip on the protein solution-functionalized surface. (c) Force curves collected at the sample data points as marked in panel b. Solid lines correspond to tip approaching process, and the dotted lines correspond to tip retraction process. (d) Histogram of maximum adhesion force as a function of the frequency of observed force, summarized from 405 non-zero data points in the FV image (panel b).

between an NGF-modified AFM tip and a surface modified with TrkA-containing protein mixture. At each pixel on the image, the tip approached and retracted from the surface to complete a force curve measurement. The rupture force, the maximum force at the moment of tip–sample detachment, is taken as a measure of the specific interaction at any point [14–26]. Due to the large volume of information recorded at each pixel, the total number of pixels in a FV image (32×32=1024) is much less than that in a regular topographic image (512×512=2.62×10^5) because of memory limitation. Thus, the resolution of a FV image is relatively low; however, the information of the tip–sample interaction at each pixel is available. When the NGF-modified tip approaches an area with TrkA, an excess adhesion force is observed as a result of the specific NGF–TrkA interaction. As the tip scanned on a 1×1 μm^2 area, a total of 1024 force curves were collected to generate the FV image. Each pixel corresponds to an average area of 31×31 nm^2. The bright–dark contrast in a FV image reflects the relative strength of the tip–sample interaction at any local region. Fig. 3c shows three typical force curves collected at the marked locations in Fig. 3b; the coloration of the pixel reflects the maximum negative deflection of this curve. The adhesion forces in the FV image fall in the range of 0–1.7 nN, among which 60% of the force curves show no adhesive peak (the bright area, e.g., (iii)), indicating the absence of TrkA. Some of the forces are well above the noise and background level, for example, a typical force of 0.08 nN at location (ii) with grey contrast; or strong adhesion force indicated by dark pixels (e.g., 1.44 nN at location (i)) ascribed to local concentration of TrkA. A histogram of the frequency of observed adhesion forces (the rest 40%) is normalized and shown in Fig. 3d, with a maximum centered at 0.06 nN. Multiples of this force also roughly appear as peaks in the histogram with rapidly diminishing intensities. Thus, we infer that 0.06 nN represents the force needed to rupture the binding between the NGF–TrkA dimer complex as to be further analyzed in Section 4.

In the control experiment, sufficient NGF solution was introduced to the solution bathing the TrkA-modified substrate prior to the force mapping. Fig. 4a shows the corresponding FV image. Multiple force curves, randomly picked across the surface (cross marks in Fig. 4a), were shown in Fig. 4b. When compared to Fig. 3c, the adhesion forces measured in Fig. 4b are negligible, indicating free NGF is able to effectively abolish binding to the NGF-modified on AFM tip. This provides strong evidence that the strong adhesive peak in force curves measured between an NGF-modified tip and a TrkA containing surface (Fig. 3c) are specific and biologically relevant. Though besides TrkA, another NGF receptor, p75, exists on PC12 cell, its binding affinity to NGF is significantly lower than TrkA [6,39–41]. The use of TrkA-specific antibody in purification also effectively excluded p75 in the protein solution. In our experiments, the contribution from p75 is neglected.

Fig. 4c shows the histogram of all the adhesion forces collected from Fig. 4a. More than 90% of the force curves show no adhesive peak, whereas the highest detectable force is 0.03 nN. Similar results have been achieved from other samples. This force is used as a convenient estimate of the maximum non-specific binding force, and any force higher is considered to be indicative of NGF–TrkA-specific interaction. Therefore the histogram in Fig. 3d indicates 34% of the surface was covered by TrkA proteins, slightly higher than the 25% of TrkA in the extracted cell surface protein solution presumably due to the variation in surface adhesion among the different proteins.

Though the TrkA functionalized sample surface is different and greatly simplified when compared to a cell surface, it provides a model system to examine the NGF–TrkA interaction and allowed us to further study the specific interaction in living cells.

3.3. Force mapping on living PC12 cells

Fig. 5 shows a set of data obtained on the surface of a living PC12 cell mapped with an NGF-modified AFM tip. Fig. 5a and b are 10×10 μm^2 height and FV images collected simultaneously. Note that both the height image and the FV image were collected at 32 pixels per line, due to the limitation of memory space. While the height image provides the surface morphological information, the FV

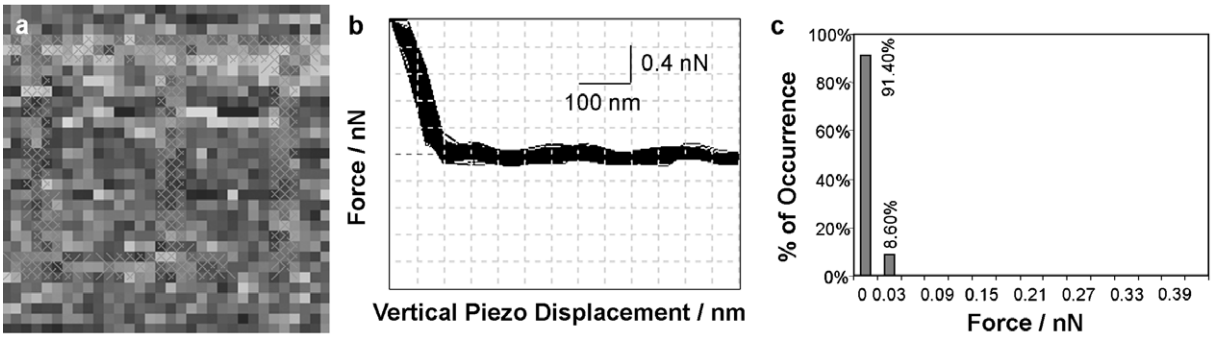

Fig. 4. (a) A 1×1 μm^2 FV image acquired by an NGF-modified tip after introducing sufficient NGF to the solution bathing the protein solution functionalized substrate. (b) Force curves randomly collected at the sample data points as cross-marked in panel a. (c) Histogram of maximum adhesion force as a function of the frequency of observed force, summarized from 1024 data points in the FV image (panel b).

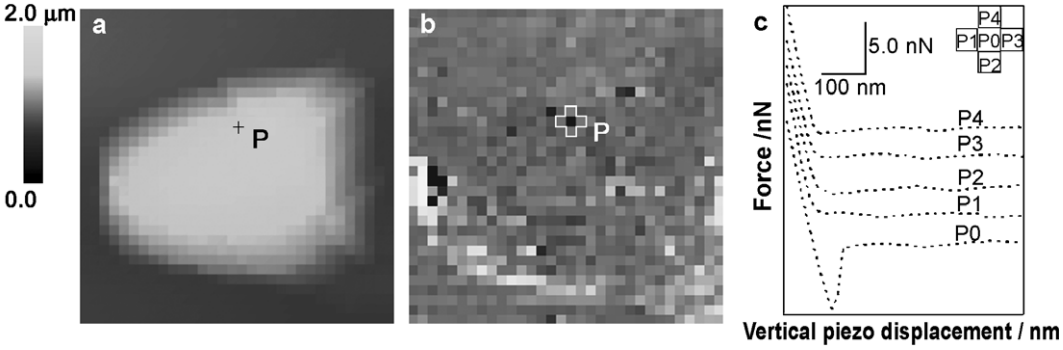

Fig. 5. (a) A 9.8×9.8 μm^2 height image acquired by an NGF-modified tip on living PC12 cell with 32 pixels per line resolution. (b) FV image captured simultaneously with the height image in panel a. (c) Force curves collected at the local region P vicinity, as marked in panels a and b, during tip retraction.

image provides a force map based on the interaction between the tip and the cell surface. The cell is about 1.6 μm in height, and 8.2×6.6 μm^2 in size. Analogous to the results acquired on the model surface (Fig. 3), the cell exhibited a heterogeneous surface in the FV image (Fig. 5b). For instance, at region P, the central pixel (P0) shows dark contrast corresponding to strong adhesion force (Fig. 5c), whereas the surrounding pixels (P1–P4) show relatively light contrast indicating fairly weak adhesion forces.

Similar data were acquired on various cells. Fig. 6 shows another set of data obtained on a separate cell mapped with an NGF-modified AFM tip. Simultaneously collected 8×8 μm^2 height and FV images are shown in Fig. 6a and b. The cell is about 1.5 μm in height, and 13.5×7.0 μm^2 in size. Similarly, the cell exhibited a heterogeneous surface with areas of no (A), weak (B), or strong (C) adhesion force. Force curves from these three regions are given in Fig. 6c. Region C shows an area with significantly dark contrast in the FV image (Fig. 6b). Thus we focused our study at this location. Four high-force pixels can be resolved in the FV image, and each pixel corresponds to an average area of 250×250 nm^2. The actual area per pixel may be larger due to the cell surface roughness. The force curves are illustrated in Fig. 6c, and peak adhesion forces of 2.87, 2.27, 1.21 and 1.13 nN were measured at the C1, C2, C3 and C4 pixels, respectively.

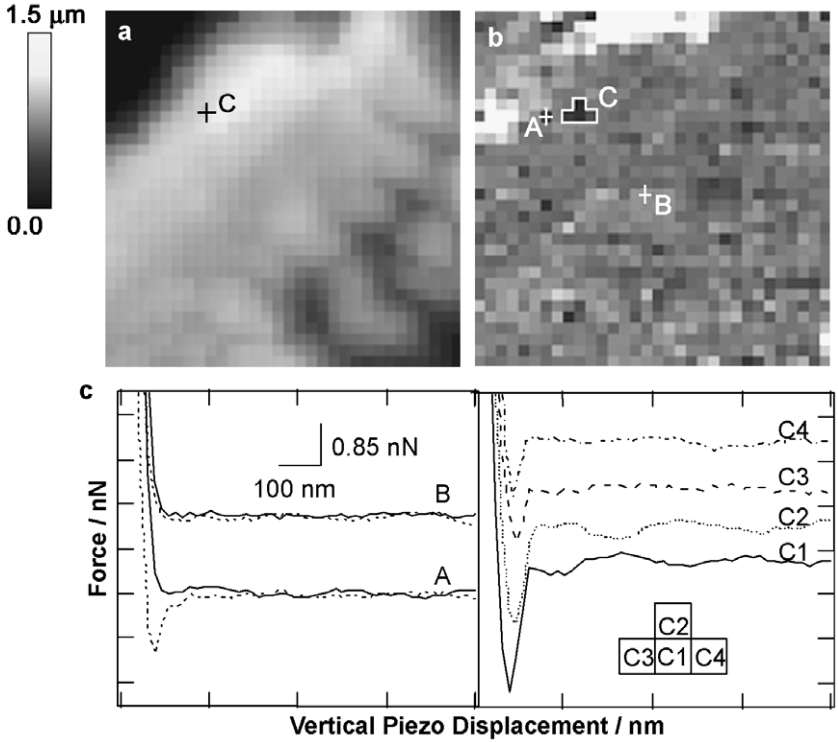

Fig. 6. (a) A 8×8 μm^2 height image acquired by an NGF-modified tip on living PC12 cell with 32 pixels per line resolution. (b) FV image captured simultaneously with the height image in panel a. (c) Force curves collected at the sample data points A and B as denoted in panel b. Solid lines correspond to tip approaching process, and the dotted lines correspond to tip retraction process. The right panel shows force curves collected at the local region C during tip retraction.

To further resolve the forces at this location, higher resolution 4×4 μm^2 images were captured. Fig. 7a and b are the height and FV images collected simultaneously. Region M in this image corresponds to region C in Fig. 6. In this image, each pixel has an approximate area of 125×125 nm^2. Sixteen force curves (Fig. 7d) were illustrated, corresponding to 16 individual pixels at this local region. The magnitude of the forces is the same as those shown in Fig. 6 even though this image was acquired 40 min after the image in Fig. 6. The reproduction of the force curves at the same region indicates the measured forces correspond to the rupture forces of NGF–TrkA interaction instead of the extraction of TrkA from the cell membrane. It provides further evidence that the specific binding force is unique and reproducible and can be used to identify and characterize protein species on a living cell. The dark columns in Fig. 7c show the histogram of the adhesion forces measured in the FV image of Fig. 7b. Among all the force measurements across the sample area, 38.6% shows non-adhesion force. The most frequently observed force is 0.1 nN, with a broad

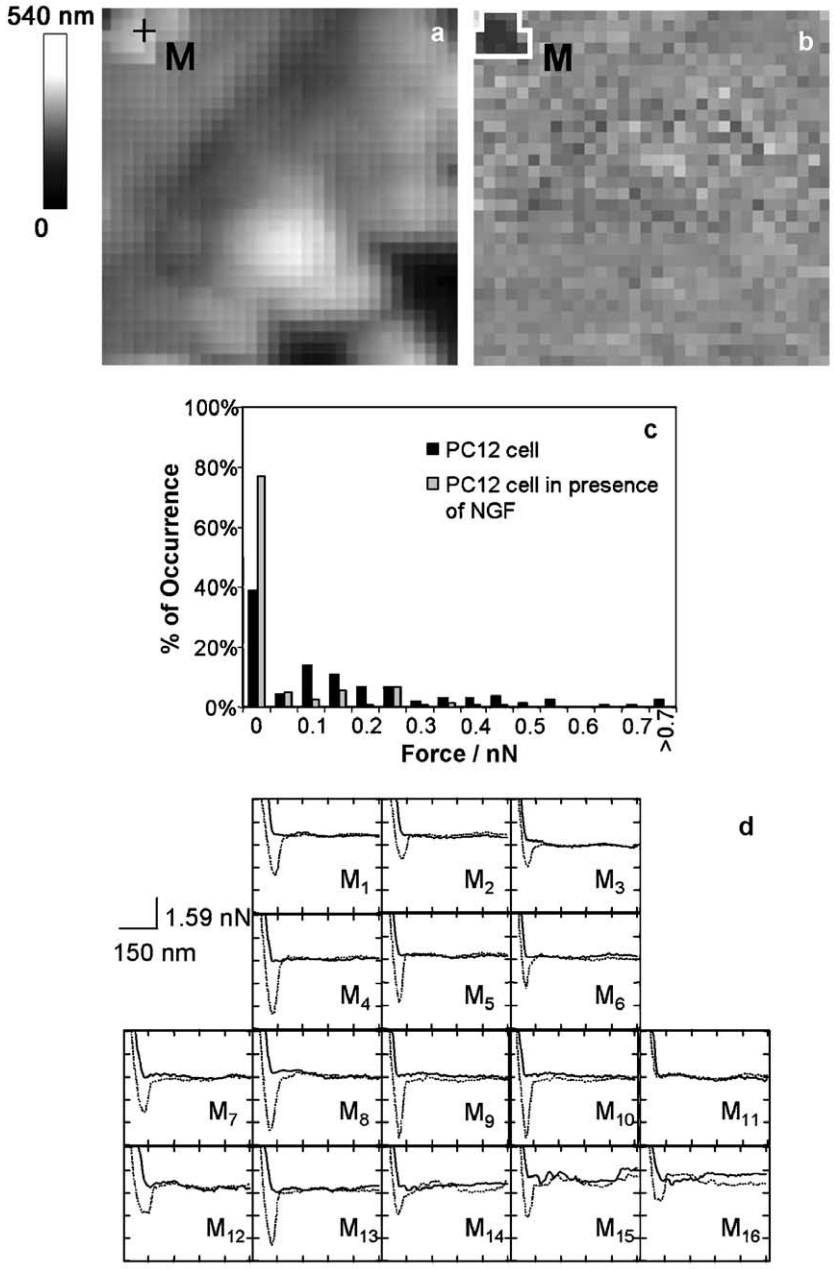

Fig. 7. (a) A 4×4 μm^2 height image acquired by an NGF-modified tip on living PC12 cell with 32 pixels per line resolution. (b) FV image captured simultaneously with the height image in panel a. (c) Histograms of maximum adhesion force as a function of the frequency of observed force, summarized from data points in the FV image (panel b) shown as black columns, and Fig. 8b shown as grey columns. (d) Force curves collected at the local region M, as marked in panels a and b. Region M is the same location as region C in Fig. 6. Solid lines: approaching; dotted lines: retraction.

distribution in the magnitude of the rest rupture forces. Among the 2.5% of pixels with forces above 0.7 nN, the majority was collected at region M. The highest observed force (e.g., 4.4 nN at M_9 and 4.3 nN at M_{10}) is approximately 70 times higher than the specific binding force of NGF–TrkA dimer complex (0.06 nN), as identified on the model sample surface (Fig. 3). It is also 2.6 times of the highest force measured in the model system (Fig. 3). The above results imply: (1) the high forces measured on cell correspond to multiple NGF–TrkA interactions, i.e., each pixel contains numeral TrkA receptors (which is reasonable when considering that each pixel is approximately 125×125 nm^2); (2) TrkA receptors form aggregates, resulting in multiple binding event at some local regions (e.g., region M); (3) additional adhesion force may be generated, in addition to the specific ligand–receptor interactions, due to the nature of cell membrane.

There are many other factors than the specific binding force that may contribute to the adhesion force measured at each pixel. For example, the tip indentation to the soft cell membrane may cause adhesion force; the cytoskeletal structure and surface roughness can affect the adhesion force by varying the surface homogeneity; NGF may weakly (non-specific) interact with other species involved in cell membrane. These forces and influences remain when sufficient NGF solution (7 nM final concentration in the cell, more than 100 times the K_d of 10^{-11} M) was introduced to the cell and occupied all the available TrkA binding sites; however, the NGF–TrkA specific interaction was excluded. Fig. 8a and b show the results of this experiment. As can be seen from the FV image, the adhesion forces were largely abrogated. Multiple force curves were randomly selected from presentation in Fig. 8c, and they clearly show no significant and characteristic interactions of the type seen in Fig. 7d. The histogram plotted based on 328 force curves collected on top of the cell is shown as the grey columns in Fig. 7c. Only 23% of the force curves show detectable adhesion forces. Among all the cells that we studied in a similar way, the highest detectable force in the control experiments is less than 0.44 nN. We consider the 0.44 nN adhesion force as the upper limit of non-specific interaction in living cells. Note that the surface roughness of cells with or without 30 min incubation with NGF maintains the same level. This excludes the possibility that the lack of high adhesion forces in the control experiments is due to the change in cell surface convolution in response to NGF injection. Thus the high adhesion forces measured in Figs. 6 and 7 were generated from the TrkA–NGF specific interaction.

4. Discussions

4.1. The strength of NGF–TrkA-specific interaction

In the model system, TrkA containing cell surface proteins were chemically bound to a substrate. These TrkAs were registered by the NGF-modified tip. As shown in the histogram in Fig. 3d, 34% force curves show adhesion forces above 0.03 nN, the level of non-specific interaction as defined in the control experiment (Fig. 4). The most probable adhesion force was measured to be 0.06 nN. The periodic appearance of its multiples of forces as peaks in the histogram allows us to tentatively consider 0.06 nN as the specific binding force between NGF and TrkA dimer. According to the SEM image of gold-coated Si_3N_4 tip, the nominal tip radius is approximately 15 nm, which can accommodate approximately 47 NGF molecules (the cross-sectional area of NGF dimer is ~5×3 nm^2) [38,42]. It is reported that when NGF binds to TrkA, a dimer of NGF–TrkA complexes forms, with an area of the extracellular portion of 9.5×3.1 nm^2 [42]. Because each pixel corresponds to an average area of 976 nm^2 on the force map, the maximum number of dimer complexes involved in the tip–sample interaction is estimated to be 33. Adhesion force as high as 1.7 nN was observed. If we assume this force correlates to the maximum number of NGF–TrkA interaction, the average rupture force of an NGF–TrkA dimer is 0.05 nN, which is in good agreement with the most probable 0.06 nN force observed in our model system. Indeed, accurate measurement of the binding strength between a biomolecular pair relies on the systematic study on the relation between the rupture force and the tip withdrawal

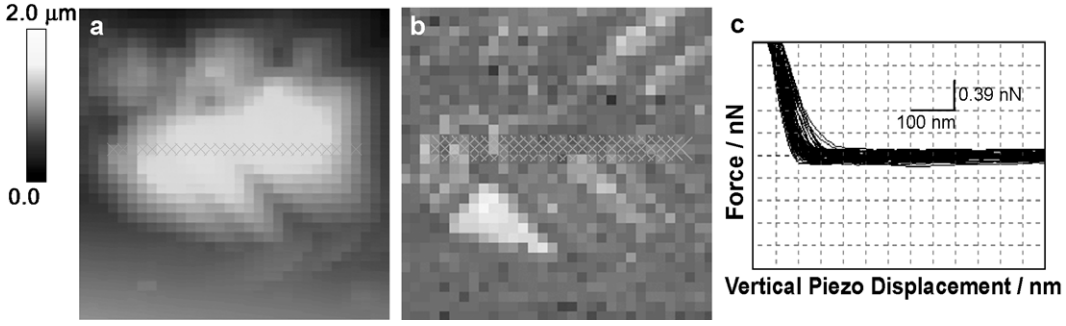

Fig. 8. (a) A 9×9 μm^2 height image of a PC12 cell acquired by an NGF-modified tip after introducing NGF into the solution bathing PC12 cells for 30 min. (b) FV image captured simultaneously with the height image in panel a. (c) Force curves randomly collected at the sample data points as cross-marked in panels a and b.

rate because bond breaking is thermally activated [46]. However, the rupture forces measured at 1 Hz show broad distribution (Figs. 3d and 7c) indicating the detection of multiple binding events at local regions. Multiple binding events are only detectable when sufficient interaction time is provided (in terms of the tip withdrawal rate) to allow the ligands on the AFM tip to adjust their orientations, diffuse to the binding sites of the receptors and bind to the receptors forming strong specific bonds [27]. In this case, the measured rupture forces can provide a reasonable estimate of the specific interaction for distinguishing the binding species from the others. The specific binding force was similarly measured between protein–ligand, antigen–antibody and complementary oligonucleotides in model systems [14–26]. In our previous study, we quantified the specific interaction between CTB and its receptor ganglioside GM1 is of 0.15 nN [27]. Typical specific binding force falls in the range of 10^{-11} to 10^{-9} N. The 0.06 nN binding force between NGF and TrkA dimer falls well within this range.

NGF–TrkA binding force in a living cell may be greater than the force in our model system. The model system is relatively rigid and not dynamic, and that the chemically anchored TrkA molecules are fixed on the surface. On cell membrane, the living cell presents TrkA in a conformation designed to efficiently interact with NGF: its extracellular binding domain pointing out, and the non-binding cytosolic portion deeply inserted in the cell membrane. This natural conformation of TrkA on cell membrane optimizes the NGF–TrkA binding. As shown in the histogram in Fig. 7c, the detectable forces are peaked at 0.1 nN with a broad distribution in magnitude. Based on our estimation of 0.44 nN as an upper limit of non-specific interaction, we can't conclude that 0.1 nN represents the NGF–TrkA specific binding force in living cells. In analogous AFM studies, Lehenkari and Horton [28] estimated a binding force of 0.127 nN for the interaction between the F11 antibody and the $\alpha_v\beta_3$ integrin dimer on freshly isolated rat osteoclasts; Osada et al. [29] suggested a binding force of 0.05 nN between lectin and GalNAc on the rat vomeronasal epithelium; Gad et al. [8] reported the binding force between concanavalin A and mannan on a yeast cell is in the range of 0.075–0.2 nN. The binding force between NGF and TrkA dimer on a living cell might be higher than 0.06 nN, as estimated in the model system, due to the favorable receptor conformation on cell membrane as well as the more deformable and complex membrane structure. However, the comparison with the reported values of specific interaction between various biomolecular pairs in living cells allows us to infer that forces greater than 0.44 nN are most likely corresponding to multiple binding events.

Besides TrkA, NGF has another cell membrane receptor, p75. Its binding affinity is 100 times lower than TrkA, and its population is three times higher [6,39–41]. When an NGF-modified tip scans on cell membrane, both TrkA and p75 give rise to adhesion force during tip retraction. However, the adhesion force generated from NGF–p75 interaction is negligible when comparing with that from NGF–TrkA interaction due to the low affinity of p75. It was reported recently that the co-expression of TrkA and p75 is required for the formation of high-affinity NGF-binding sites, and they are presumably composed of p75–TrkA heteromers [37,40,41]. Though our current study did not address this issue, this may also be partly responsible for the much greater forces seen on the living cells compared to the model system, where p75 is absent. We expect to answer this question by generating force maps using modified AFM tips with TrkA-specific and p75-specific antibodies.

4.2. TrkA distribution

We have utilized the NGF–TrkA specific interaction to probe TrkA distribution. While NGF is considered to induce receptor dimerization as a first step for signal transduction [47,48], our observation supports the report by Mischel et al. [49], in which the freeze-fracture electron microscopic analysis demonstrated that TrkA tends to form oligomers even in the absence of NGF.

The FV imaging identifies 0.06 nN as the specific interaction between the NGF and TrkA dimers in the model system. If dimer is the dominant form of TrkA in the model system, we expect to observe a narrow band in the histogram. The broad distribution of the measured forces as shown in Fig. 3d rules out this possibility. Forces above 0.06 nN, especially the multiples of 0.06 nN, indicate the detection of multiple binding events. Multiple binding events can only be probed when multiple receptors are highly localized, suggesting the existence of TrkA aggregates.

Analogous results were obtained on the living cell membrane as demonstrated in Fig. 7c. According to the 0.44 nN upper limit of non-specific interaction, higher forces on the force map (Fig. 7b) suggest the detection of multiple binding events at local regions. The uneven darkness of the TrkA containing pixels in Figs. 5b, 6b and 7b indicates TrkA must aggregate with distinct number at individual pixel. This is consistent with the broad distribution of the measured forces in living cells in the histogram (Fig. 7c), suggesting that the TrkA aggregates may vary in size. For instance, region M in Fig. 7b shows the darkest contrast in the force map, indicating numeral TrkAs highly localize at the vicinity of "M". At this region, TrkA distribution is further resolved, with pixels M4, M5, M8, M9, M10 and M13 exhibiting the highest forces. These forces are each distinct and reproducible, indicating that placing the tip over each point provided access to different numbers of TrkA molecules.

The height image (Fig. 7a) shows a distinct, elevated surface feature at the same region. We speculate cell membrane may be convoluted in this local area. When TrkAs locally exist at this area, the convolution further condenses the receptors resulting in a larger number of receptors per unit area. Receptor proteins can migrate along the cell surface [50] and the cell membrane is more

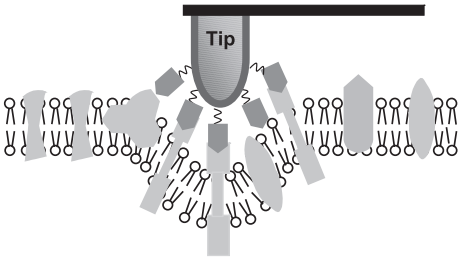

Fig. 9. Illustration of cell membrane deformation in response to NGF-modified tip approaching, resulting in multiple NGF–TrkA bindings.

deformable. In response to the NGF-modified tip approaching, the cell membrane may conform to partially envelop the tip, allowing TrkAs in the vicinity available for simultaneous binding to the ligands on the tip (Fig. 9). The multiple ligand–receptor interactions lead to greater adhesion forces, implying the higher level of receptor clustering in living cells. In fact, the surface of the cell membrane is about 10 times rougher than the surface of the protein-modified surface in our model system, causing an average of 6% increase in surface area partially due to the membrane convolution. It is thus reasonable to observe much higher adhesion forces on the living cell membrane.

It should be noted that the effect of cell membrane convolution is valid only when TrkA aggregates exist at the local region. The total number of TrkA per PC12 cell is only 1.5×10^4 [39]. If the receptors are uniformly dispersed as monomers on the membrane of the cell (in Figs. 6 and 7) with a dimension of $13.5\times7.0\times1.5$ μm^3, the average area per receptor is estimated to be 130×130 nm^2, approximately the area per pixel in the force map of Fig. 7b. If this is the case, much less multiple binding events should be observable due to the 15 nm nominal radius of the AFM tip even if we count the membrane convolution. In fact, the same type of strong adhesion force also appears at relatively flat regions, and is lacking at other elevated regions. Therefore, the cell membrane convolution does not downgrade our conclusion of TrkA aggregation on the cell membrane. When comparing the simultaneously captured height image and force map (Figs. 5a and b, 6a and b, or 7a and b), it is found that the distribution of TrkA aggregates is random and is irrelevant to the cell membrane topography.

Our study suggests that receptor distribution on living cell surface can be explicitly examined with a ligand-modified AFM tip. It is expected, while FV images are captured at smaller and smaller scales and focused on high adhesion force region, the receptor aggregates can be more carefully studied. Due to the simplicity and uniformity in the local environment, we expect that the non-specific interaction can be greatly reduced and eventually individual receptors will be pinpointed on the cell surface. Detachment of PC12 cells from the substrate prevented us from capturing higher resolution images. However, our work laid the foundation of further exploring this novel methodology.

5. Conclusions

We have employed the NGF–TrkA specific interaction as a probe to register TrkA distribution on living PC12 cell. NGF–TrkA specific interaction was first studied in a model system, where NGF was chemically bound to an AFM tip, and partially purified TrkA was chemically bound onto a substrate. Specific binding force between NGF–TrkA dimer was quantified at 0.06 nN. TrkA in the protein mixture was identified by an NGF-modified tip via the specific interaction. Similar but stronger interactions were observed on living PC12 cells. Force maps generated by scanning an NGF-modified AFM tip across the living cell illustrated the distribution of TrkA. The distribution is heterogeneous, with TrkA highly localized at certain regions. This aggregation is consistent with its signaling function as an NGF receptor. It is expected that force mapping at smaller scales will eventually allow us to pinpoint the individual receptors due to the greatly simplified surface environment at the local cell membrane. Our methodology offers a general approach for studying cell surface protein distribution in living cells in a natural environment.

Acknowledgements

This work is supported by National Science Foundation (IBN-0103080).

References

[1] E. Henderson, P.G. Haydon, D.S. Sakaguchi, Actin filaments dynamics in living glial cells imaged by atomic force microscopy, Science 257 (1992) 1944–1946.
[2] J.H. Hoh, C.A. Schoenenberger, Surface morphology and mechanical properties of MDCK monolayers by atomic force microscopy, J. Cell. Sci. 107 (1994) 1105–1114.
[3] F. Braet, C. Rotsch, E. Wisse, M. Radmatcher, Comparison of fixed and living liver endothelial cells by atomic force microscopy, Appl. Phys., A 66 (1997) S575–S578.
[4] F.M. Ohnesorge, J.K.H. Horber, W. Haberle, C.P. Czerny, D.P.E. Smith, G. Binnig, AFM review study on pox viruses and living cells, Biophys. J. 73 (1997) 2183–2194.
[5] T.A. Camesano, M.J. Natan, B.E. Logan, Observation of changes in bacterial cell morphology using tapping mode atomic force microscopy, Langmuir 16 (2000) 4563–4572.
[6] E. Hassan, W.F. Heinz, M.D. Antonik, N.P. D'Costa, S. Nageswaran, C.-A. Schoenenberger, J.H. Hoh, Relative microelastic mapping of living cells by atomic force microscopy, Biophys. J. 74 (1998) 1564–1578.
[7] E. Lesniewska, M.C. Giocondi, V. Vie, E. Finot, J.P. Goudonnet, C. Legrimellec, Atomic force microscopy of renal cells: limits and prospects, Kidney Int. 65 (1998) S42–S48.
[8] M. Gad, A. Itoh, A. Ikai, Mapping cell wall polysaccharides of living microbial cells using atomic force microscopy, Cell Biol. Int. 21 (1997) 697–706.
[9] J.A. Callow, S.A. Crawford, M.J. Higgins, P. Mulvaney, R. Wetherbee, The application of atomic force microscopy to topographical studies and force measurements on the secreted adhesive of the green alga *Enteromorpha*, Planta 211 (2000) 641–647.

[10] M. McElfresh, E. Baesu, R. Balhorn, J. Belak, M.J. Allen, R.E. Rudd, Combining constitutive materials modeling with atomic force microscopy to understand the mechanical properties of living cells, Proc. Natl. Acad. Sci. U. S. A. 99 (2002) 6493–6497.
[11] R. Lal, B. Drake, D. Blumberg, D.R. Saner, P.K. Hansma, S.C. Feinstein, Imaging real-time neurite outgrowth and cytoskeletal reorganization with an atomic force microscope, Am. J. Physiol., Cell Physiol. 38 (1995) C275–C285.
[12] C. Rotsch, M. Radmacher, Drug-induced changes of cytoskeletal structure and mechanics in fibroblasts—an atomic force microscopy study, Biophys. J. 78 (2000) 520–535.
[13] A. Cricenti, G. De. Stasio, R. Generosi, M.A. Scarselli, P. Perfetti, M.T. Ciotti, D. Mercanti, P. Casalbore, G. Margaritondo, Native and modified uncoated neurons observed by atomic force microscopy, J. Vac. Sci. Technol., A 14 (1996) 1741–1746.
[14] G.U. Lee, L.A. Chrisey, R.J. Colton, Direct measurement of the forces between complementary strands of DNA, Science 266 (1994) 771–773.
[15] U. Dammer, M. Hegner, D. Anselmetti, P. Wagner, M. Dreier, W. Huber, H.-J. Guntherodt, Specific antigen/antibody interactions measured by atomic force microscopy, Biophys. J. 70 (1996) 2437–2441.
[16] S. Allen, J. Davies, M.C. Davies, A.C. Dawkes, C.J. Roberts, S.J.B. Tendler, P.M. Williams, The influence of epitope availability on AFM studies of antigen–antibody interactions, Biochem. J. 341 (1999) 173–178.
[17] L.T. Mazzola, C.W. Frank, S.P.A. Fodor, C. Mosher, R. Lartius, E. Henerson, Discrimination of DNA hybridization using chemical force microscopy, Biophys. J. 76 (1999) 2922–2933.
[18] L.M. Wilde, S. Allen, M.C. Davies, S.J.B. Tendler, P.M. Williams, C.J. Roberts, Bifunctional atomic force microscopy probes for molecular screening applications, Anal. Chim. Acta 479 (2003) 77–85.
[19] E.L. Florin, V.T. Moy, H.E. Gaub, Adhesion force between individual ligand–receptor pairs, Science 264 (1994) 415–417.
[20] V.T. Moy, E.L. Florin, H.E. Gaub, Intermolecular forces and energies between ligands and receptors, Science 266 (1994) 257–259.
[21] P. Hinterdorfer, W. Baumgarter, H.J. Gruber, K. Schilcher, H. Schindler, Detection and localization of individual antibody–antigen recognition events by atomic force microscopy, Proc. Natl. Acad. Sci. U. S. A. 93 (1996) 3477–3481.
[22] S. Allen, X. Chen, J. Davies, M.C. Davies, A.C. Dawkes, J.C. Edwards, C.J. Roberts, J. Sefton, S.J.B. Tendler, P.M. Williams, The detection of antigen–antibody binding events with the atomic force microscope, Biochemist 36 (1997) 7457–7463.
[23] S.S. Wong, E. Joselevich, A.T. Woolley, C.L. Cheung, C.M. Lieber, Covalently functionalized nanotubes as nanometer-sized probes in chemistry and biology, Nature 394 (1998) 52–55.
[24] P.F. Luckham, K. Smith, Direct measurement of recognition forces between proteins and membrane receptors, Faraday Discuss. 111 (1998) 307–320.
[25] D. Fotiadis, S. Scheuring, S.A. Müller, A. Engel, D.J. Müller, Imaging and manipulation of biological structures with the AFM, Micron 33 (2002) 385–397.
[26] Y. Harda, M. Kuroda, A. Ishida, Specific and quantized antigen–antibody interaction measured by atomic force microscopy, Langmuir 16 (2000) 708–715.
[27] S. Vengasandra, G. Sethumadhavan, F. Yan, R. Wang, Studies on the protein–receptor interaction by atomic force microscopy, Langmuir 19 (2003) 10940–10946.
[28] P.P. Lehenkari, M.A. Horton, Single integrin molecule adhesion forces in intact cells measured by atomic force microscopy, Biochem. BioPhys. Res. Commun. 259 (1999) 645–650.
[29] T. Osada, S. Takezawa, A. Itoh, H. Arakawa, M. Ichikawa, A. Ikai, The distribution of sugar chains on the vomeronasal epithelium observed with an atomic force microscope, Chem. Senses 24 (1999) 1–6.
[30] M. Horton, G. Charras, P. Lehenkari, Analysis of ligand–receptor interactions in cells by atomic force microscopy, J. Recept. Signal Transduct. 22 (2002) 169–190.
[31] H. Kim, H. Arakawa, T. Osada, A. Ikai, Quantification of cell adhesion force with AFM: distribution of vitronectin receptors on a living MC3T3-E1 cell, Ultramicroscopy 97 (2003) 359–363.
[32] M.V. Sofroniew, C.L. Howe, W.C. Mobley, Nerve growth factor signaling, neuroprotection, and neural repair, Annu. Rev. Neurosci. 24 (2001) 1217–1281.
[33] C. Wiesmann, A.M. de Vos, Nerve growth factor: structure and function, Cell. Mol. Life Sci. 58 (2001) 748–759.
[34] G.J. Siegel, N.B. Chauhan, Neurotrophic factors in Alzheimer's and Parkinson's disease brain, Brain Res. Rev. 33 (2000) 199–227.
[35] N.F. Schor, Signal transduction for clinicians: why should we care? Pediatr. Neurol. 25 (2001) 361–367.
[36] C.F. Ibáñez, Neurotrophic factors: from structure–function relationships to designing effective therapeutics, Trends Biotechnol. 3 (1995) 217–227.
[37] S. Maliartchouk, H.U. Saragovi, Optimal nerve growth factor trophic signals mediated by synergy of TrkA and p75 receptor-specific ligands, J. Neurosci. 17 (1997) 6031–6037.
[38] N.Q. McDonald, R. Lapatto, J. Murray-Rust, J. Gunning, A. Wlodawer, T.L. Blundell, New protein fold revealed by a 2.3-Å resolution crystal structure of nerve growth factor, Nature 354 (1991) 411–414.
[39] S.E. Buxser, L. Watson, G.L. Johnson, A comparison of binding properties and structure of NGF receptor on PC12 pheochromocytoma and A875 melanoma cells, J. Cell. Biochem. 22 (1983) 219–233.
[40] B.L. Hempstead, D. Martin-Zanca, D.R. Kaplan, L.F. Parada, M.V. Chao, High-affinity NGF binding requires coexpression of the trk proto-oncogene and the low-affinity NGF receptor, Nature 350 (1991) 678–683.
[41] M.V. Chao, B.L. Hempstead, p75 and TrkA: a two-receptor system, Trends Neurosci. 18 (1995) 321–326.
[42] C. Wiesmann, M.H. Ultsch, S.H. Bass, A.M. de Vos, Crystal structure of nerve growth factor in complex with the ligand-binding domain of the TrkA receptor, Nature 401 (1999) 184–188.
[43] M.H. Ultsch, C. Wiesmann, L.C. Simmons, J. Henrich, M. Yang, D. Reilly, S.H. Bass, A.M. de Vos, Crystal structures of the neurotrophin-binding domain of TrkA, TrkB and TrkC, J. Mol. Biol. 290 (1999) 149–159.
[44] R. Wang, S. Vengasandra, F. Yan, Probing the nature of cholera toxin B oligomer by the atomic force microscopy, Chem. Lett. 11 (2001) 1170–1171.
[45] F. Yan, L.-H. Chen, Q.-L. Tang, R. Wang, Synthesis and characterization of a photo-cleavable cross-linker and its application on tunable surface modification and protein photo-delivery, Bioconj. Chem., in communication.
[46] R. Merkel, P. Nassoy, A. Leung, K. Ritchie, E. Evans, Using dynamic force spectroscopy to explore energy landscapes of receptor–ligand bonds, Nature 397 (1999) 50–53.
[47] S.O. Meakin, E.M. Shooter, Molecular investigations on the high-affinity nerve growth factor receptor, Neuron 6 (1991) 153–163.
[48] J. Schlessinger, A. Ullrich, Growth factor signaling by receptor tyrosine kinases, Neuron 9 (1992) 383–391.
[49] P.S. Mischel, J.A. Umbach, S. Eskandari, S.G. Smith, C.B. Gundersen, G.A. Zampighi, Nerve growth factor signals via preexisting TrkA receptor oligomers, Biophys. J. 83 (2002) 968–976.
[50] R. Wang, J. Shi, A.N. Parikh, A.P. Shreve, L. Chen, B.I. Swanson, Evidence for cholera aggregation on GM1 decorated lipid bilayers, Colloids Surf., B Biointerfaces 33 (2004) 45–51.